Differential Targeting of Glucosylceramide and Galactosylceramide Analogues after Synthesis but Not during Transcytosis in Madin-Darby Canine Kidney Cells

Ida van Genderen and Gerrit van Meer

Department of Cell Biology, Faculty of Medicine and Institute of Biomembranes, University of Utrecht, 3584 CX Utrecht, The Netherlands

Abstract. A short-chain analogue of galactosylceramide (6-NBD-amino-hexanoyl-galactosylceramide, C_6-NBD-GalCer) was inserted into the apical or the basolateral surface of MDCK cells and transcytosis was monitored by depleting the opposite cell surface of the analogue with serum albumin. In MDCK I cells 32% of the analogue from the apical surface and 9% of the analogue from the basolateral surface transcytosed to the opposite surface per hour. These numbers were very similar to the flow of membrane as calculated from published data on the rate of fluid-phase transcytosis in these cells, demonstrating that C_6-NBD-GalCer acted as a marker of bulk membrane flow. It was calculated that in MDCK I cells 155 μm^2 of membrane transcytosed per cell per hour in each direction. The fourfold higher percentage transported from the apical surface is explained by the apical to basolateral surface area ratio of 1:4. In MDCK II cells, with an apical to basolateral surface ratio of 1:1, transcytosis of C_6-NBD-GalCer was 25% per hour in both directions. Similar numbers were obtained from measuring the fraction of endocytosed C_6-NBD-GalCer that subsequently transcytosed. Under these conditions lipid leakage across the tight junction could be excluded, and the vesicular nature of lipid transcytosis was confirmed by the observation that the process was blocked at 17°C. After insertion into one surface of MDCK II cells, the glucosylceramide analogue C_6-NBD-GlcCer randomly equilibrated over the two surfaces in 8 h. C_6-NBD-GalCer and -GlcCer transcytosed with identical kinetics. Thus no lipid selectivity in transcytosis was observed. Whereas the mechanism by which MDCK cells maintain the different lipid compositions of the two surface domains in the absence of lipid sorting along the transcytotic pathway is unclear, newly synthesized C_6-NBD-GlcCer was preferentially delivered to the apical surface of MDCK II cells as compared with C_6-NBD-GalCer.

EPITHELIAL cells form tight monolayers. These monolayers are sealed by the tight junctions, a continuous zone of cell to cell contacts surrounding the apex of each cell. The tight junctions divide the plasma membrane of differentiated epithelial cells into an apical and a basolateral domain that differ in protein and lipid composition (Simons and van Meer, 1988; Rodriguez-Boulan and Nelson, 1989), and they prevent random diffusion of molecules between the underlying tissue and the external milieu. Nevertheless, many different molecules must pass across epithelial cell monolayers. This transport is often mediated by receptors and occurs via membrane vesicles by a process termed transcytosis.

Transcytosis from the basolateral to the apical domain appears also to be required for generating the cell-surface polarity of apical glycoproteins in some cells like hepatocytes and intestinal cells (Hubbard et al., 1989). Kidney-derived MDCK cells, however, sort most newly synthesized plasma membrane proteins before they reach the surface. Still, even in MDCK cells a subset of plasma membrane proteins transcytoses bidirectionally between the two surface domains (Brändli et al., 1990). So, at each surface, epithelial cells face the task of sorting molecules destined for transcytosis from resident molecules. Studies on transcytosis of endogenous and transfected transmembrane receptors have provided insight in the sorting steps and the required sorting signals (for reviews see Mellman et al., 1993; Mostov and Cardone, 1995). The first step in transcytosis is endocytosis. Endocytosed apical membrane reaches endosomes underlying the apical membrane. Basolateral endocytotic vesicles fuse into a separate set of basolateral endosomes. Although endocytosis provides a first sorting step at the cell surface, actual sorting between molecules to be retained and molecules to be transcytosed

Address all correspondence to Gerrit van Meer, Department of Cell Biology, Faculty of Medicine and Institute of Biomembranes, AZU HO2.314 Universiteit Utrecht, 3584 CX Utrecht, The Netherlands. Tel.: 31-30506480. Fax: 31-30541797. E-mail: g.vanmeer@pobox.ruu.nl

occurs in the endosomes. In the simplest case, sorting could involve the same signals to discriminate apical from basolateral molecules in apical and basolateral endosomes and even in the TGN along the exocytotic pathway (Matter et al., 1993; Aroeti and Mostov, 1994). By modifying the signal after arrival at the plasma membrane, a molecule could be directed to one domain during exocytosis and transcytosed to the opposite domain when the need arises (Song et al., 1994). Recent evidence, however, has suggested that the hierarchy of these signals in the TGN may be different from that in the endosomes implying that the sorting machineries of TGN and endosomes are related but not identical (Aroeti et al., 1993).

Clearly, the rates of endocytosis and recycling that have been measured for transmembrane glycoproteins depend on signals and do not reflect rates of bulk membrane flow. As targeting information may be present in the cytoplasmic, transmembrane, and exoplasmic domain of the protein, even proteins lacking a cytoplasmic tail cannot be considered signal-free. In contrast to fluid-phase markers, markers of membrane flow have not yet been reported for the transcytotic transport route. Therefore, absolute efficiencies of sorting, i.e., enrichment of a membrane component as compared with membrane flux (van Genderen and van Meer, 1993) remain to be established for transcytosis.

Like proteins, the various lipid classes are distributed unequally over the two surfaces of epithelial cells (see Simons and van Meer, 1988). Based on the presence of a barrier to lipid diffusion in the exoplasmic but not in the cytoplasmic leaflet of the plasma membrane bilayer, it has been concluded that the differences in lipid composition reside in the exoplasmic leaflet. The cytoplasmic leaflet of the two domains is thought to possess an identical lipid composition (Simons and van Meer, 1988). A series of studies has demonstrated that newly synthesized analogues of the sphingolipids sphingomyelin (SM)[1] and glucosylceramide (GlcCer) reach the epithelial cell surface with a different apical/basolateral polarity (van Meer et al., 1987; van Meer and van't Hof, 1993) that accurately reflected the surface polarity of the endogenous SM and GlcCer found in intestinal cells (van't Hof and van Meer, 1990; van't Hof et al., 1992). It was expected that to maintain the different lipid compositions of their two surface domains, cells should sort lipids along the transcytotic pathway as well.

The rationale behind the present study was to measure transcytosis of lipid molecules that have a different surface polarity in epithelial cells. GlcCer displays a twofold higher apical/basolateral polarity than galactosylceramide (GalCer) in MDCK cells (Nichols et al., 1988). By several experimental approaches, all using short-chain fluorescent (C_6-NBD) analogues of GalCer and GlcCer (Lipsky and Pagano, 1985), it is shown that these lipids were transcytosed. Unexpectedly, the lipids followed bulk membrane flow, and were not sorted from each other during transcytosis. Using this property, the transcytotic membrane flux could be determined. In contrast to the absence of sorting in the transcytotic pathway, after synthesis by the cell 6-NBD-amino-hexanoyl-glucosylceramide (C_6-NBD-GlcCer) was enriched on the apical cell surface as compared with C_6-NBD-GalCer.

1. *Abbreviations used in this paper*: C_6-NBD-, 6-NBD-amino-hexanoyl-; GalCer, galactosylceramide; GlcCer, glucosylceramide; HBSS′, HBSS without bicarbonate and phenol red with 10 mM Hepes, pH 7.2; HBSS′ + BSA, HBSS′ containing 1% (wt/vol) BSA; SM, sphingomyelin.

Materials and Methods

Materials

BSA fraction V was purchased from Sigma Chemical Co. (St. Louis, MO). Randomly labeled L-[^{3}H]serine (22 Ci/mmol) was from New England Nuclear (Boston, MA). Cell culture plastics and filters were from Costar Corp. (Cambridge, MA). Chemicals, silica TLC plates, and solvents were of analytical grade and obtained from Riedel-de Haën (Seelze, FRG).

Cell Culture

The MDCK cell clones strain I (Fuller et al., 1984) and strain II (Louvard, 1980) were obtained from K. Simons, European Molecular Biology Laboratory, Heidelberg, FRG. Cells were cultured on 24.5-mm-diam polycarbonate filters glued to the base of a plastic ring, the filter holder (Transwell, Costar Corp.), as described (van Genderen et al., 1991). The ring separates the apical medium on top of the filter inside the ring, from the basal medium underneath the filter and outside the ring. Confluent monolayers were used for experiments three or four days after seeding. Under these conditions, one filter contained 3.8×10^6 MDCK I cells (Parton et al., 1989) and $(4.7–5) \times 10^6$ MDCK II cells (van Genderen et al., 1991; van't Hof et al., 1992). The cells were free of mycoplasma in an assay using Hoechst DNA stain 33258 (Sigma Chemical Co.).

Lipid Preparation and Analysis

C_6-NBD-ceramide was obtained from Molecular Probes (Eugene, OR). C_6-NBD-GalCer, C_6-NBD-GlcCer, and C_6-NBD-SM were synthesized from NBD-hexanoic acid (Molecular Probes) and psychosine, glucopsychosine, and sphingosylphosphorylcholine (Sigma Chemical Co.), respectively, as before (van Meer et al., 1987). Products were purified by TLC in chloroform/acetone/methanol/acetic acid/water (50:20:10:10:5, vol/vol), where NBD-hexanoic acid runs to the front and the products lag behind. Retention factor (R_f) values for C_6-NBD-GalCer, -Glc, and -SM were 0.5, 0.5, and 0.1. The identity of the products was further confirmed by sensitivity to β-galactosidase but not α-galactosidase (C_6-NBD-GalCer) and sphingomyelinase. C_6-NBD-GlcCer was positively identified by colocalization with the NBD product that was synthesized from NBD-ceramide in a strictly UDP-glucose-dependent reaction by a membrane pellet of CHO cells, which do not have the ability to synthesize C_6-NBD-GalCer.

For analysis, lipids were extracted from media and cells into chloroform/methanol (Bligh and Dyer, 1959; van't Hof and van Meer, 1990). Products were identified by a TLC procedure devised to separate GalCer from both GlcCer and SM. 10×10 cm^2 TLC plates were dipped in 2.5% borate (wt/vol) in methanol (Kean, 1966) and dried. The lipid extract was applied and the plates were first developed in chloroform/methanol/25% (wt/vol) ammonia/water (65:35:4:4, vol/vol), followed by chloroform/acetone/methanol/acetic acid/water (50:20:10:10:5, vol/vol) for the second direction. R_f values for C_6-NBD-GalCer, -Glc, and -SM were 0.3, 0.5, and 0.3 in the first direction, 0.5, 0.5 and 0.1 in the second direction. Fluorescent spots were quantified in a fluorimeter after scraping the fluorescent spots from the plate and extracting the lipids from the silica as described (van't Hof and van Meer, 1990).

Radiolabeled spots were detected by fluorography after dipping the TLC plates in 0.4% 2, 5 diphenyloxazol PPO in 2-methylnaphthalene with 10% xylene. Preflashed film (X-Omat S; Eastman Kodak Co., France) was exposed to the TLC plates for 3 d at −80°C. Radioactive spots representing SM, GlcCer and GalCer were identified by iodine staining of standards that had been added to the extract before TLC. They were scraped from the plates and the radioactivity was quantified by liquid scintillation counting in 0.3 ml Solulyte (J. T. Baker Chemicals, Deventer, The Netherlands) and 3 ml of Ultima Gold (Packard Instruments, Downers Grove, IL). A blank spot on the experimental TLC plate contained 13 Bq.

Liposomes (26 nmol NBD-lipid/ml) or NBD-lipid/BSA complexes (5 μM lipid, 5 μM BSA [0.03% wt/vol]) were prepared in HBSS without bicarbonate and phenol red buffered with 10 mM Hepes, pH 7.2 (HBSS′) as before (van Meer et al., 1987; van't Hof and van Meer, 1990).

Assays for Delivery of NBD Lipids to the Cell Surface

Unidirectional Transcytosis of Exogenous C_6-NBD-GalCer and C_6-NBD-GlcCer (Fig. 1 A). Cells were washed with HBSS′ and incubated at 10°C for 30 min in a 6-well cluster dish with on one surface C_6-NBD-GalCer and C_6-NBD-GlcCer, simultaneously (2.5 μM each) or separately (5 μM), complexed to BSA (Fig. 1 *A*1). Standard vols were 1 ml apically and 1.5 ml basolaterally. After removal of the NBD lipid, the cells were incubated at 37°C with HBSS′ on the side of insertion and with a 1% (wt/vol) solution of BSA (HBSS′ + BSA) on the opposite side to extract NBD lipid into the medium immediately upon its arrival (Fig. 1 *A*2). After varying time intervals the NBD lipid remaining on the surface of insertion was recovered by BSA extractions (BSA washes) for 20 min at 10°C in HBSS′ + BSA (Fig. 1 *A*3). Including the 37°C BSA extraction, two BSA extractions were performed for the apical and three for the basal side. NBD lipids from the combined apical media, the combined basal media, and the cells were extracted into chloroform/methanol, analyzed by two-dimensional TLC, and quantitated.

Incorporation of each NBD lipid into the apical and basal surface was ~40 and 120 pmol for MDCK I, and 80 and 160 pmol for MDCK II per filter, which for some reason does not exactly correspond with the relative surface areas of the two cell lines. With a surface area of 90 $Å^2$ for a phospholipid–cholesterol pair (Demel and de Kruijff, 1976), the apical and the basolateral surface of an MDCK II monolayer (1,165 μm^2/cell, 3.5×10^6 cells/filter; Butor and Davoust, 1992) contain 10 nmol phospholipid–cholesterol equivalents each. Thus, the inserted NBD lipid would represent 1–2% of the polar lipids on each surface. In MDCK I this would be <1%.

Transcytosis of Exogenous C_6-NBD-GalCer after Endocytosis (Fig. 1 B). C_6-NBD-GalCer was inserted at 10°C as above (Fig. 1 *B*1). Cells were rinsed three times with cold HBSS′ and incubated at 37°C in HBSS′ to allow endocytosis (Fig. 1 *B*2). After 10 min, C_6-NBD-GalCer remaining on the cell surface was removed by two (apical) or three (basal) BSA washes for 20 min at 10°C (Fig. 1 *B*3). At this stage, one set of filters was used for lipid analysis to quantitate endocytosis. A second set of filters was further incubated for 0.5 or 1 h at 37°C in HBSS′ + BSA, to assay for reappearance of intracellular C_6-NBD-GalCer on either cell surface (Fig. 1 *B*4). These incubations were followed by a 10°C BSA wash, after which the NBD lipids from the combined apical media, basal media, and the cells were extracted into chloroform/methanol, analyzed by TLC, and quantitated. The percentage of C_6-NBD-GalCer transcytosed per hour was calculated as (percent endocytosis per hour) × (the fraction of intracellular C_6-NBD-GalCer that was transcytosed). Endocytosis (intracellular plus transcytosed after 10 min) was somewhat underestimated because recycling of C_6-NBD-GalCer to the membrane of insertion during the endocytosis incubation (Fig. 1 *B*2) could not be measured. On the other hand, it was overestimated because transcytosis during this incubation was not corrected for leakage.

Equilibration of Exogenous C_6-NBD-GlcCer (Fig. 1 C). Cells were incubated for 30 min at 10°C with 5 μM C_6-NBD-GlcCer, complexed to BSA, in either the apical or basal HBSS′ (Fig. 1 *C*1). Cells were then rinsed with cold HBSS′ three times, and incubated in the CO_2 incubator at 37°C in a chemically defined, serum-free medium (Fuller et al., 1984) without BSA containing 50 μM conduritol B-epoxide as an inhibitor of lysosomal glucocerebrosidase (Fig. 1 *C*2). After 8–16 h the incubations were stopped by cooling the cells, after which the C_6-NBD-GlcCer residing on each surface was assayed by BSA washes for 20 min at 10°C, two for the apical, and three for the basal side (Fig. 1 *C*3).

Delivery of Newly Synthesized Sphingolipids to the Cell Surface (Fig. 1 E). Cells were incubated at 37°C with 5 μM NBD-ceramide/BSA complexes in both apical and basal media (Fig. 1 *E*1). After 15 min, BSA in HBSS′ was added to both media to yield HBSS′ + BSA, 1.5 ml apical, 2 ml basal (Fig. 1 *E*2). At 90 min after the start of the 37°C incubation the media were collected. Two additional BSA washes were performed on both sides for 30 min at 10°C. Lipids from the combined apical media, the combined basal media, and from the cells were then extracted into chloroform/methanol. For each lipid the apical/basolateral polarity of transport to the cell surface was calculated by dividing the amount of that lipid in the apical media by the amount in the basal media. The relative polarity for two lipids was calculated as the quotient of their apical/basolateral polarities, and is proportional to the apical enrichment of the one lipid as compared to the other (van 't Hof and van Meer, 1990).

To study the temperature dependence of transport, NBD-ceramide (5 μM) in 1 ml HBSS′ + BSA was added apically for 2 h at 10°C, followed by a second incubation in HBSS′ + BSA without ceramide for 1 h at 10°C. The subsequent transport incubation was carried out in HBSS′ + BSA. It was followed by a 30 min 10°C BSA-wash. Two time points (separate filters, in duplicate) were selected for each temperature to ascertain that the transport rate was measured in the linear range of the assay: 1 and 2 h at 10, 15, and 20°C; 0.5 and 1 h at 25 and 30°C; 20 and 40 min at 37°C. Data were calculated from the earliest time point and are expressed as transport per 30 min.

Equilibration of Endogenously Synthesized C_6-NBD-GlcCer and C_6-NBD-SM (Fig. 1 F). Equilibration of newly synthesized C_6-NBD-GlcCer and -SM over the two cell surfaces, measured at 37°C in media without BSA,

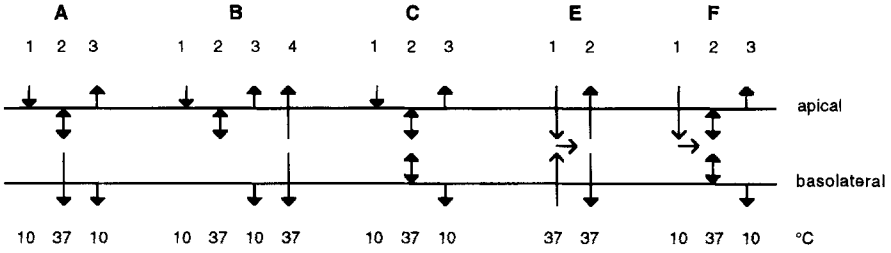

Assay (see text)	1 C_6-NBD-lipid added	Side	2 BSA	3, 4 BSA	C_6-NBD-lipid depleted
A (D)	GalCer / GlcCer	ap (or bl)	bl (or ap)	ap + bl	GalCer / GlcCer
B	GalCer	ap	no	ap + bl	GalCer
C	GlcCer	ap (or bl)	no	ap + bl	GlcCer
E	ceramide	ap + bl	ap + bl		GlcCer / GalCer / SM
F	ceramide	ap	no	ap + bl	GlcCer / SM

Figure 1. Essential features of the assays *A–F* used in the text to measure the delivery of NBD lipids to the two cell surfaces. An NBD lipid unable to cross the plasma membrane was inserted into the cell surface in step 1 (*short arrows*, *A*, *B*, and *C*). The long thin arrow in E and F indicates that C_6-NBD-ceramide crosses the plasma membrane and diffuses into the cytoplasm. The horizontal arrow reflects conversion of the ceramide to sphingolipid products. In step 2, the cells were incubated at 37°C to allow lipid transport. Double-headed arrows indicate equilibration of the sphingolipid between the cell surface(s) and endocytotic organelles in the absence of BSA. Appearance of C_6-NBD-GalCer, -GlcCer, and -SM on either cell surface was monitored by an extraction using BSA in step 2 (*arrows* into the medium in assays *A* and *E*) or was measured in a subsequent incubation with BSA at 10°C in step 3 (*arrows* into the medium in assays *A*, *B*, *C*, and *F*). In assay B, this was followed by step 4, a transport incubation at 37°C with BSA extraction into the medium (*arrows*). *ap*, apical; *bl*, basolateral.

was compared with their first arrival on the cell surface measured in media containing BSA, as described (van't Hof and van Meer, 1990). Monolayers of MDCK II cells were incubated with NBD-ceramide in liposomes apically for 30 min at 10°C (Fig. 1 *F*1). During the subsequent incubation for 1 h at 37°C, NBD products appearing on the apical and basolateral cell surface were either trapped by extraction into HBSS' + BSA as in Fig. 1 *E*2, or, alternatively, allowed to endocytose and transcytose in the absence of BSA (Fig. 1 *F*2). In the latter case, the resulting surface polarity for each lipid was assayed by two subsequent BSA washes at 10°C (Fig. 1 *F*3). While in the experiment with BSA the 37°C media contained 71 ± 6% and the 10°C media contained 11 ± 3% of the C_6-NBD-GlcCer plus -SM, the 37°C medium without BSA contained 5 ± 1%, and the subsequent 10°C BSA wash contained 60 ± 5% in four experiments (n = 8). Synthesis of both C_6-NBD-GlcCer and -SM was roughly six times less than in Table III. Two filters were combined for each analysis. The amount of C_6-NBD-GalCer in this type of experiment was below the detection limit (<1 pmol/2 filters).

Results

Unidirectional Transcytosis of Exogenous C_6-NBD-GalCer

To assay for lipid transcytosis we inserted a fluorescent lipid analogue into the apical surface of MDCK cells and monitored appearance on the opposite cell surface (Fig. 1 *A*). For this, we used an analogue of GalCer, an endogenous lipid in MDCK cells (Brändli et al., 1988; Nichols et al., 1988), carrying an NBD hexanoic acid (C_6-NBD-GalCer). Such C_6-NBD lipids can be efficiently inserted into the outer leaflet of the plasma membrane at low temperature (10°C) and can be extracted from the surface by the addition of an excess of BSA (1% wt/vol) to the medium (Lipsky and Pagano, 1985; van Meer et al., 1987). After insertion of C_6-NBD-GalCer into the apical plasma membrane at 10°C and removal of excess C_6-NBD-GalCer (Fig. 1 *A*1), the cells were warmed to 37°C with BSA in the medium on the opposite side to trap any C_6-NBD-GalCer appearing on the basolateral surface (Fig. 1 *A*2). After cooling to 10°C, BSA was added to the apical side to extract C_6-NBD-GalCer present on the apical surface after the 37°C incubation and to the basolateral side as a BSA wash (Fig. 1 *A*3). As shown in Fig. 2, C_6-NBD-GalCer was transcytosed to the basolateral surface of MDCK I and II cells at a rate of 32 and 25% per hour, respectively. Transcytosis in the opposite direction was also observed. Remarkably, transcytosis of C_6-NBD-GalCer in MDCK I was much slower from basolateral to apical, while in MDCK II transcytosis was similar in both directions.

MDCK I cells grown on polycarbonate filters display a ratio between apical and basolateral surface area of 1:4 (Parton et al., 1989; Butor and Davoust, 1992). In a confluent monolayer of epithelial cells the absolute amount of membrane transported in both directions must be equal (as has been documented for fluid phase; von Bonsdorff et al., 1985; Bomsel et al., 1989). When expressed as percentage of the membrane of origin, in MDCK I this would require transcytosis of a fourfold higher percentage from the apical surface than from the basolateral surface. This was typically observed for the transcytosis of C_6-NBD-GalCer (Fig. 2). After an initial lag, basolateral to apical transcytosis of C_6-NBD-GalCer reached a maximum rate of 8.6% per hour. The maximal (initial) rate of transcytosis from the apical surface was about four times higher, 32.2% per hour. So, in MDCK I cells, C_6-NBD-GalCer was transcytosed with the relative rates of bulk membrane flow.

Interestingly, in MDCK II cells grown on polycarbonate filters the ratio of apical to basolateral surface area has been reported to be 1:1 (van Genderen et al., 1991; Butor and Davoust, 1992). With equal absolute amounts of membrane being transported in both directions, in MDCK II cells the same percentage of the apical membrane area must be transcytosed per hour as the percentage of the basolateral surface area that is transcytosed per hour. This

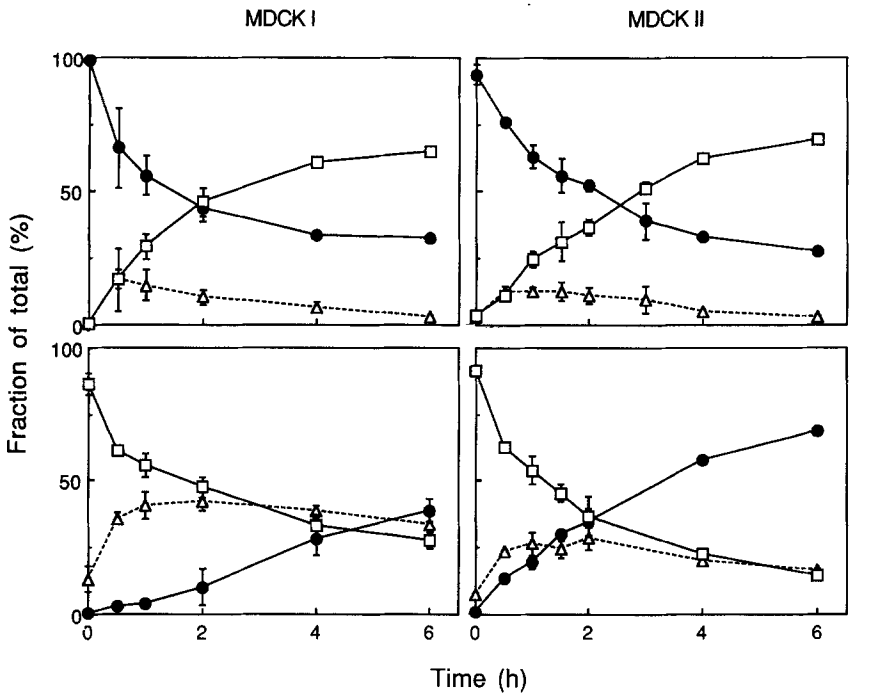

Figure 2. Transcytosis of C_6-NBD-GalCer in MDCK I (*left*) and MDCK II cells (*right*). After insertion of C_6-NBD-GalCer into the apical surface (*top*) or the basolateral surface (*bottom*) at 10°C, cells were incubated at 37°C with BSA in the opposite medium. After the indicated time intervals, the medium was collected and BSA washes were performed at 10°C. Lipids from cells (△), the combined apical media (●), and the combined basal media (□) were quantified. Data are the mean of the average values in three to five experiments. Error bars, SD.

was indeed found (Fig. 2). C_6-NBD-GalCer thus followed bulk flow also in MDCK II cells.

Transcytosis of Exogenous C_6-NBD-GalCer After Endocytosis

As an independent assay for the rate of lipid transcytosis, we followed the fate of endocytosed C_6-NBD-GalCer. From measuring (*a*) the percentage of inserted C_6-NBD-GalCer that was endocytosed per hour and (*b*) the fraction of the endocytosed C_6-NBD-GalCer that reached the opposite surface, the percentage of inserted C_6-NBD-GalCer that reached the opposite surface per hour could be calculated. For this, exogenous C_6-NBD-GalCer was inserted into one cell surface at 10°C (Fig. 1 *B*1) and endocytosis was allowed in the absence of BSA for 10 min at 37°C (Fig. 1 *B*2). Subsequently, endocytosis was determined in one set of filters by BSA extraction of C_6-NBD-GalCer in the cold from each cell surface and quantitation of fluorescence in the media and in the cells (Fig. 1 *B*3). A second set of filters was warmed to 37°C for 1 h with BSA present in both apical and basal medium, and reappearance of endocytosed lipid on the two cell surfaces was measured. Typical experiments for MDCK I and II are shown in Table I. In MDCK I, endocytosis from the apical surface, scored as the sum of intracellular C_6-NBD-GalCer plus C_6-NBD-GalCer present on the basolateral surface, was 19.7% in 10 min. 28.8% of the cellular C_6-NBD-GalCer was transported to the basolateral side during the subsequent hour. From these numbers, 34% of the C_6-NBD-GalCer inserted into the apical surface was transcytosed per hour. Endocytosis from basolateral was 24.9% in 10 min, and 7.1% of the cellular C_6-NBD-GalCer was transported to the apical side, resulting in basolateral to apical transcytosis of 11% per hour. The kinetics are in good agreement with those measured in the direct transcytosis assay (see Fig. 2).

Similar data were obtained in three experiments where transcytosis of endocytosed C_6-NBD-GalCer was measured in MDCK II cells. Endocytosis from the apical surface was 17% after 10 min. 33 ± 7% of endocytosed C_6-NBD-GalCer was transported to the basolateral side. Endocytosis from basolateral was 37% in 10 min, and 13 ± 2% of the endocytosed C_6-NBD-GalCer was transported to the apical side. From these numbers, 33 ± 7% of the C_6-NBD-GalCer inserted into the apical surface was transcytosed per hour to the basolateral surface ($n = 4$). In the opposite direction this was 32 ± 2% per hour ($n = 4$). These kinetics are again similar to those measured in the direct transcytosis assay.

The ratio of transcytosis toward the opposite surface versus recycling back to the membrane of insertion could be calculated from the measurements of reappearance on the cell surface. For MDCK I this ratio was 1:2 after apical insertion, 1:10 after basolateral insertion. For MDCK II these numbers were 1:1 and 1:5, respectively. The extent of reappearance in MDCK II was assayed by incubating filters for 0.5 and 1 h at 37°C. After 30 min, a total of 78% of apically and 85% of basolaterally endocytosed C_6-NBD-GalCer had reappeared on the cell surface, which increased to 88% and 93% after 1 h: very little C_6-NBD-GalCer remained in the cells.

*Table I. Endocytosis of C_6-NBD-GalCer after Apical or Basolateral Insertion and Reappearance at the Two Surface Domains**

Compartment	C_6-NBD-GalCer distribution after endocytosis (10 min 37°C)		Subsequent redistribution of cellular C_6-NBD-GalCer (1 hr 37°C) in HBSS' + BSA	
	(Percentage of inserted)		*(Percentage of total)*	
	MCDK I	II	MDCK I	II
After apical insertion				
Cells	14.1	11.6	16.6	14.4
Apical medium	80.3	82.6	54.7	49.4
Basolateral medium	5.6	5.8	28.8	36.2
Total (pmol/filter)	*25*	*74*	*5*	*7*
After basolateral insertion				
Cells	23.6	28.4	12.6	8.1
Apical medium	1.3	8.5	7.1	15.0
Basolateral medium	75.1	63.1	80.3	76.9
Total (pmol/filter)	*111*	*99*	*30*	*30*

*C_6-NBD-GalCer was inserted into one surface of MDCK cells at 10°C as described in Materials and Methods (Fig. 1 *B*1). Endocytosis was then allowed to occur for 10 min at 37°C (Fig. 1 *B*2). Subsequently, the C_6-NBD-GalCer was extracted from the apical and basolateral surfaces at 10°C by BSA (Fig. 1 *B*3), and endocytosed C_6-NBD-GalCer was calculated as percentage of total C_6-NBD-GalCer inserted. In a parallel incubation, the cells were further incubated in HBSS' + BSA for 1 h at 37°C (Fig. 1 *B*4) to allow reappearance of the internalized C_6-NBD-GalCer at the cell surface. This was followed by a 10°C BSA wash, after which media and cells were analyzed for C_6-NBD-GalCer. Data represent the mean of typical experiments in duplicate with a range ≤5% for MDCK I and ≤10% for MDCK II.

Equilibration of Exogenous C_6-NBD-GlcCer

As an independent assay for studying whether or not a glycolipid followed bulk membrane flow during transcytosis, we inserted an NBD lipid into one cell surface, allowed equilibration over the two surface domains at 37°C in the absence of BSA, and measured the resulting distribution over the two surfaces by a BSA extraction in the cold (Fig. 1 *C*). When C_6-NBD-GalCer was used, a high percentage was hydrolyzed by the cells during the 8–16 h time course of these experiments. Hydrolysis after 16 h as estimated from the amount of C_6-NBD-SM at the end of the experiment was 30–40% (NBD-ceramide, the immediate product of C_6-NBD-GalCer hydrolysis, was efficiently metabolized to C_6-NBD-SM). Therefore, we used C_6-NBD-GlcCer in the presence of conduritol B-epoxide, a specific and irreversible inhibitor of lysosomal glucocerebrosidase (van Weely et al., 1993). Conduritol B-epoxide reduced the amount of C_6-NBD-SM formed to 6% at the end of the incubation. Unfortunately, conduritol B-epoxide did not adequately prevent C_6-NBD-GlcCer degradation in MDCK I, where 30% C_6-NBD-SM was found after 16 h.

After 8–16 h, 30% of the C_6-NBD-GlcCer was found on both the apical and the basolateral surface of MDCK II cells with 40% inside the cell (Table II). The equilibrium distribution reached after insertion of C_6-NBD-GlcCer into the apical cell surface was the same as after basolateral insertion. In both cases the final apical/basolateral polarity was 1, which equals the ratio of apical to basolateral surface area in these MDCK II cells (see above). So exogenous C_6-NBD-GlcCer assumed the distribution of bulk membrane. No selectivity was observed during transcytosis of this lipid either.

*Table II. Steady State Distribution of C_6-NBD-GlcCer after Apical or Basolateral Insertion in MDCK II Cells**

Side of insertion	Percentage of total C_6-NBD-GlcCer			Surface polarity (apical/basolateral)
	Cellular	Apical	Basolateral	
Apical‡	41.4 ± 5.9	29.7 ± 2.0	28.9 ± 4.4	1.04 ± 0.11
Basolateral	42.2 ± 10.1	28.2 ± 2.8	29.6 ± 7.6	0.98 ± 0.14

*C_6-NBD-GlcCer was inserted into either the apical or basolateral surface of MDCK II cells at 10°C as described in Materials and Methods (Fig 1 *C*1). Cells were then incubated in serum-free medium without BSA in the CO_2 incubator at 37°C (Fig. 1 *C*2). After 8–16 h, the NBD lipids were extracted from the apical and basolateral surfaces by BSA at 10°C (Fig. 1 *C*3), and quantitatively analyzed. Data are the mean ± SD of five experiments with varying incubation times: 8 h (3 exp.), 10 h, and 16 h.

‡After insertion into the apical surface ~15% of the NBD lipid was found to be sticking to the inside of the filter holder in an experiment where the filter was cut from the holder after the 8–16 h incubation and the holder extracted with BSA separately. The apical signal was corrected for this. If the same correction would apply to the experiments shown in Figs. 2 and 3, and Table I (which represent raw data), apical to basolateral transcytosis has been underestimated by a factor 1.2.

Unidirectional Transcytosis of Exogenous C_6-NBD-GalCer versus C_6-NBD-GlcCer

For a direct comparison of the rates of transcytosis for C_6-NBD-GalCer and -GlcCer, exogenous C_6-NBD-GalCer and -GlcCer were inserted simultaneously into the apical cell surface at 10°C, after which transcytosis was monitored at 37°C as described above (Fig. 1 *A*). The same experiment was performed in the opposite direction. In MDCK II cells, 25% of the C_6-NBD-GlcCer that had been inserted was transcytosed to the opposite surface in 1 h. This was the same in both directions. Moreover, the rates were remarkably similar for C_6-NBD-GalCer (Fig. 3). The same results were obtained when the lipids had been added to separate filters, or when NBD-lipid concentrations were lowered 50 times (data not shown). Also in MDCK I cells transcytosis of C_6-NBD-GalCer was directly compared with that of C_6-NBD-GlcCer by simultaneous insertion. In two experiments during 2 h, transcytosis was identical for C_6-NBD-GlcCer and C_6-NBD-GalCer in both directions and followed the kinetics displayed for C_6-NBD-GalCer in Fig. 2 (data not shown).

Differential Ttransport of C_6-NBD-GalCer and C_6-NBD-GlcCer after Biosynthesis

In contrast to C_6-NBD-GalCer and -GlcCer, NBD-ceramide inserted into the plasma membrane readily translocates to the cytosolic leaflet because of the absence of a polar head group. From there, it exchanges through the cytoplasm to the Golgi complex where it serves as a substrate for SM synthase and glycosyltransferases (Fig. 1 *E*1 and *F*1). These processes proceed at temperatures down to 0°C (van Helvoort et al., 1994). When, at higher temperature, the resulting NBD-lipid products reach the cell surface, they can be immediately extracted quantitatively into the incubation medium by BSA (van Meer et al., 1987; Fig. 1 *E*2). Alternatively, in the absence of BSA they will equilibrate with the endocytic membranes and with the opposite cell surface (Fig. 1 *F*2). Subsequently, NBD lipids on the cell surface can be extracted at low temperature with a BSA-containing medium (Fig. 1 *F*3).

When MDCK II cells were incubated with NBD-ceramide on both sides at 37°C, C_6-NBD-GlcCer and -SM were synthesized in amounts that were 7.5-fold higher than when the ceramide had been added apically at 10°C, the former routine procedure (van Meer et al., 1987). Under these conditions, C_6-NBD-GlcCer reached the cell surface with an apical/basolateral polarity of 1.4, and C_6-NBD-SM with a polarity of 0.7. The relative polarity of C_6-NBD-GlcCer/C_6-NBD-SM, the ratio of the polarities, was 2.2 (Table III). The apical/basolateral polarity for each lipid in the present experiment, where ceramide was supplied to both cell surfaces, is intermediate between the polarity measured after apical addition alone and the polarity after basolateral addition alone (discussed in van Meer

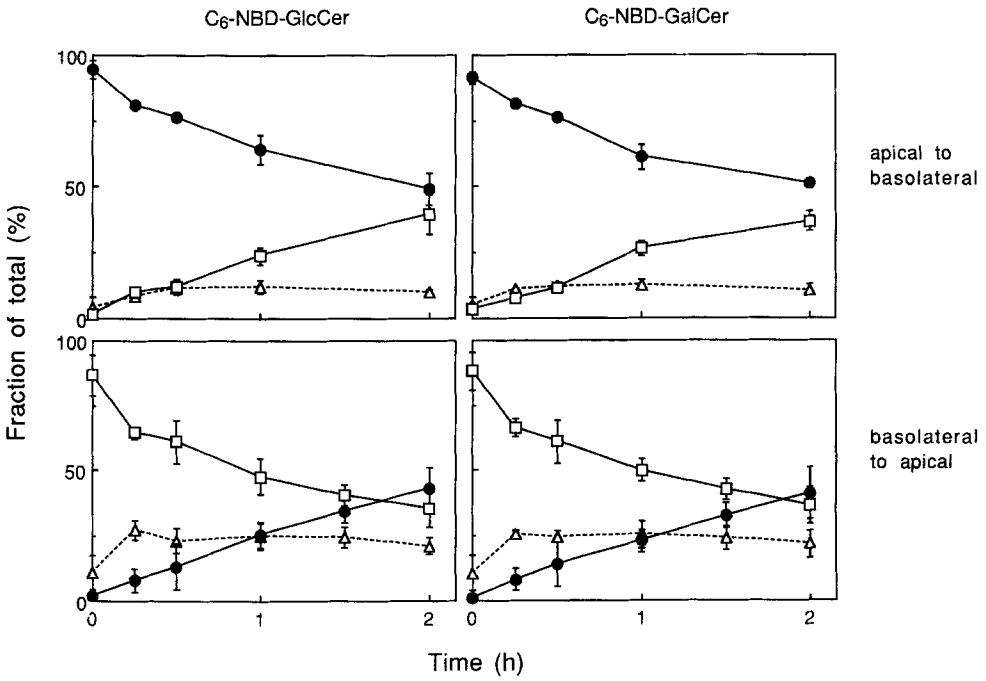

Figure 3. Transcytosis of C_6-NBD-GlcCer (*left*) and C_6-NBD-GalCer (*right*) in MDCK II cells. After simultaneous insertion of the two NBD lipids into the apical surface (*top*) or the basolateral surface (*bottom*) at 10°C as described in the legend to Fig. 2, the cells were incubated at 37°C with BSA in the opposite medium. After the indicated time intervals, the medium was collected and BSA washes were performed at 10°C. Lipids from cells (△), the combined apical media (●), and the combined basal media (□) were quantified. Data are the mean of four (apical insertion) or six (basolateral insertion) measurements in two and three experiments. Error bars, SD.

*Table III. Delivery of Newly Synthesized C_6-NBD-lipids to the Surface of MDCK II Cells**

C6-NBD-lipid	Apical/basolateral polarity		Relative polarity (polarity/polarity)
GlcCer	1.43 ± 0.13	C_6-NBD-GlcCer/GalCer	2.56 ± 0.32
GalCer	0.57 ± 0.17	C_6-NBD-GlcCer/SM	2.24 ± 0.20
SM	0.66 ± 0.16		

*Monolayers of MDCK II cells were incubated with C_6-NBD-ceramide on both sides for 1.5 h at 37°C (Fig. 1 *E*1). After the first 15 min, 1% BSA was added to both media and NBD products appearing on either cell surface were trapped by the BSA in the medium (Fig. 1 *E*2). After two additional BSA washes at 10°C, C_6-NBD-GlcCer, -GalCer, and -SM in both media and in the cells were quantitatively analyzed, and apical/basolateral polarities of delivery were calculated as described under Materials and Methods. Synthesis was 320 pmol C_6-NBD-SM, 40 pmol C_6-NBD-GlcCer, and 1.3 pmol C_6-NBD-GalCer per filter. Transport amounted to 82 ± 5% for all three lipids. Lipids from six filters were combined to yield reliable data on C_6-NBD-GalCer polarity. Data are the mean of two experiments in duplicate and are followed by the SD.

and van 't Hof, 1993). However, the relative polarity was ~2 in all cases and was independent of the side of ceramide addition.

Under the present conditions, for the first time also synthesis of a small amount of C_6-NBD-GalCer could be measured. During 1.5 h the relative synthesis of C_6-NBD-SM, -GlcCer and -GalCer was 100:12:0.4 (Table III). This reflects the rates of synthesis of the endogenous sphingolipids from [^{3}H]ceramide. When a 6-cm-diam dish with MDCK II cells was incubated in 2 ml complete medium containing 4 μCi [^{3}H]serine in the CO_2 incubator for 20 h, the radioactivity incorporated into SM, GlcCer, and GalCer was 3,600, 320, and 20 Bq, respectively, a ratio of 100:9:0.5. The low rate of GalCer synthesis is unexpected, as GalCer is a major glycosphingolipid in MDCK II cells (see Discussion). C_6-NBD-GalCer was delivered to the cell surface with an apical/basolateral polarity of 0.6, 2.6 times lower than that of C_6-NBD-GlcCer (Table III). So MDCK cells are able to sort these lipids after biosynthesis.

Equilibration of Endogenously Synthesized C_6-NBD-GlcCer and C_6-NBD-SM

In the transcytosis experiments, the ratio between exogenous C_6-NBD-GalCer and -GlcCer was very different from the ratio with which these lipids are synthesized by the cell. To exclude that this, or incorrect insertion, was the reason for the absence of sorting during transcytosis, we studied the equilibration of NBD lipids over the two cell surfaces after insertion in the proper ratio by the cell itself. For this, the transport assay of newly synthesized NBD lipids was adapted. After arrival on the cell surface, the newly synthesized NBD lipids were allowed to partition into the endocytotic and transcytotic pathway by omission of the BSA from the 37°C medium (Fig. 1 *F*2). In this assay, the apical/basolateral polarity of each NBD lipid at the end of the incubation was measured by a subsequent BSA extraction in the cold (Fig. 1 *F*3). The results were compared with an experiment with BSA in the 37°C medium.

The polarities of delivery of C_6-NBD-GlcCer and -SM that were generated after synthesis, as measured in a 1-h incubation in the presence of BSA, were 1.7 ± 0.7 and 0.9 ± 0.1, respectively. When endocytosis and transcytosis had occurred, in the absence of BSA, these numbers changed to 1.4 ± 0.3 and 1.1 ± 0.2, repectively; the relative polarity decreased from 1.91 ± 0.52 to 1.33 ± 0.20 (n = 8; P < 0.005). The relative polarity in the absence of BSA was not further reduced during a second hour at 37°C, but interpretation of this observation is complicated by ongoing hydrolysis and resynthesis of C_6-NBD-SM. Transcytosis seemed unable to maintain the difference between the apical/basolateral distribution for the two lipids generated by the transport from the sites of synthesis to the cell surface.

When BSA was left out of the medium of the 37°C incubation on one side only, the extent of transcytosis could be assayed by measuring how much extra product was extracted by BSA from the opposite surface, as compared with a control transport assay with BSA in both media (van 't Hof and van Meer, 1990). During 1 h at 37°C, ~20% (21 ± 7%; n = 14) of the C_6-NBD-GlcCer and -SM that reached one surface after synthesis, as measured in the control experiment, transcytosed to the opposite surface in MDCK II. This was true for both products and in both directions (data not shown) and was in the same range as the rates measured in the direct assays.

Temperature Dependence of Lipid Transcytosis

In MDCK II cells, 25% of the inserted C_6-NBD-GalCer reached the opposite cell surface in 1 h at 37°C (Fig. 4), which decreased to ~3–5%/h at 17°C. In MDCK I cells apical to basolateral transcytosis was 40% per hour at 37°C versus 3% at 17°C (n = 6). The temperature dependence of the process was compared with that of transport of newly synthesized C_6-NBD-SM from the Golgi complex to the cell surface. For this, C_6-NBD-SM synthesis was restricted to a preincubation at 10°C by applying a pulse–

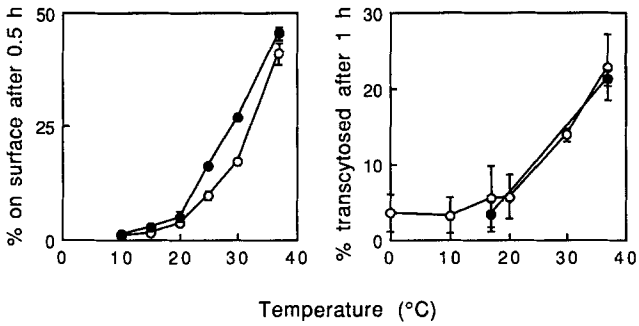

Figure 4. Temperature dependence of transport of newly synthesized C_6-NBD-SM to the cell surface and of transcytosis of C_6-NBD-GalCer. (*Left*) MDCK II cells were incubated with NBD-ceramide at 10°C before delivery of new C_6-NBD-SM to the apical (○) and to the basolateral (●) surface was measured at the various temperatures by extraction into HBSS' + BSA as described under Materials and Methods. (*Right*) After apical or basolateral insertion of C_6-NBD-GalCer at 10°C, transcytosis was measured by extraction of transcytosed C_6-NBD-GalCer by the BSA in the opposite medium; in the apical to basolateral direction (○) and, in parallel experiments, in the basolateral to apical direction (●). After additonal BSA washes at 10°C, transcytosis was determined. Transcytosis was measured during 1 and 2 h. At or below 20°C the 2-h time point was used for calculations. The 0°C experiment was completely performed on ice. Data represent the mean of two (*left*) and four (*right*) measurements. Error bars, range and SD.

chase protocol (Materials and Methods). C_6-NBD-SM that was synthesized on the cell surface was removed by the BSA in the preincubation medium before the start of the transport incubation (van Helvoort et al., 1994). The similarity between the temperature dependence of transcytosis and the transport of newly synthesized C_6-NBD-SM (Fig. 4) supported the notion that lipid transcytosis occurred by a vesicular pathway (see Discussion).

Less clear results were obtained when the effect of energy depletion was tested. In MDCK II cells, the presence of 50 mM deoxyglucose and 5 mM Na-azide (with or without preincubation with the energy poisons for 30 min at 37°C) reduced apical to basolateral transcytosis of C_6-NBD-GalCer from 25 ± 3% to 16 ± 4% per hour, with 10% inside the cell after 1 h at 37°C (n = 4). In MDCK I, transcytosis was lowered from 39 ± 2% to 18 ± 3% per hour (n = 4). However, 44 ± 2% was found in the cell after 1 h at 37°C vs. 21 ± 1% in the control. So here endocytosis seems less sensitive to energy depletion than transcytosis (and recycling). Unfortunately, under more stringent conditions the tight junctions opened as evidenced by the appearance of an NBD-lipid signal in the apical medium indicative of leakage of BSA from the basal medium.

Discussion

Transcytotic Membrane Flux

Two short-chain fluorescent glycolipid analogues, C_6-NBD-GalCer and C_6-NBD-GlcCer, were efficiently transported across a monolayer of MDCK cells at 37°C (Figs. 2–4). Leakage across the tight junctions appeared not to play a major role at 37°C, as similar rates of transepithelial transport were measured in an approach where the endocytosis and transcytosis steps were studied separately, and where all C_6-NBD-GalCer had necessarily passed through the cell (Table I). In its temperature dependence (Fig. 4) the process was very similar to endocytosis of various fluid-phase and membrane markers (Oka and Weigel, 1989; Tomoda et al., 1989), protein transcytosis (Hunziker et al., 1990; van Deurs et al., 1990; Barroso and Sztul, 1994), and exocytotic transport of C_6-NBD-SM (Fig. 4), which has to be vesicular as C_6-NBD-SM is synthesized in the Golgi lumen and does not flip across the Golgi membrane (see Koval and Pagano, 1991). These properties argue that transepithelial transport of the C_6-NBD lipids occurred by transcytosis.

C_6-NBD-GalCer and C_6-NBD-GlcCer displayed no specificity during transcytosis in MDCK cells. First of all, the relative transcytosis of C_6-NBD-GalCer and -GlcCer in the two directions, the percentage of the analogue on each surface transcytosed per hour as calculated from two different approaches (Fig. 2; Table I), closely correlated with the transcytotic flux of membrane predicted from surface area considerations in MDCK I and II cells. Second, equilibration of C_6-NBD-GlcCer in MDCK II cells resulted in a distribution that accurately reflected the relative surface area of the two domains (Table II). Under the latter conditions transport of newly synthesized NBD lipids was still selective: when after 16 h in serum-free medium without BSA NBD-ceramide was added to the cells, biosynthesis, transport, and apical/basolateral polarities were identical to those in Table III (not shown). In conclusion, the NBD sphingolipids behaved as bulk membrane markers, although so far it could not be excluded that they were transported faster (or slower) than the bulk membrane, but to the same extent in each direction.

To address this issue, the flow of membrane during transcytosis was calculated independently from literature data on the transcytosis of fluid-phase and the size of transcytotic vesicles. In MDCK I cells fluid-phase transcytosis was $2.7–3.1 \times 10^{-8}$ nl per cell per minute, as measured by HRP and FITC-dextran (von Bonsdorff et al., 1985; Bomsel et al., 1989; Prydz et al., 1992). The diameter of transcytotic vesicles immunoisolated from rat liver has been estimated to be 80 nm (Sztul et al., 1991), in agreement with the 50–100-nm profiles labeled during transcytosis in MDCK I (von Bonsdorff et al., 1985). From these numbers the transcytotic membrane flux is 122–140 μm^2 per hour per cell. With an apical surface area in MDCK I under the present growth conditions of 423–478 μm^2 and a basolateral surface area of 1,785–1,798 μm^2 (Parton et al., 1989; Butor and Davoust, 1992), 29 ± 3% of the apical membrane area and 7 ± 1% of the basolateral surface area transcytose per hour. These numbers are very similar to the transcytosis of C_6-NBD-GalCer (Fig. 2) and demonstrate that this analogue acted as a true marker of bulk membrane flow.

MDCK II cells display apical and basolateral surface areas of 1,189 and 1,141 μm^2 (Butor and Davoust, 1992), a ratio similar to, for example, that for the proximal nephron in vivo (Welling and Welling, 1975). Using C_6-NBD-GalCer as a marker (Figs. 2 and 3), ~300 μm^2 of membrane was transcytosed per MDCK II cell per hour in each direction, two times more than in MDCK I.

For dimeric IgA, the ligand of the polymeric Ig receptor (Mostov and Deitcher, 1986), and for a mutant polymeric Ig receptor (Casanova et al., 1990) a half-time of basolateral to apical transcytosis was measured of 30 min in MDCK. This is much shorter than the half-time of transcytosis of membrane which is on the order of 6 and 3 h in MDCK I and II, respectively (Fig. 2). A different mutant polymeric Ig receptor was found to be preferentially recycled which resulted in a half-time of transcytosis of >10 h (Casanova et al., 1990). Clearly, proteins can be actively concentrated into the transcytotic pathway or into the recycling pathway, which can now be directly measured by applying the present methodology.

Membrane Endocytosis and Recycling

C_6-NBD-SM behaved as a bulk flow marker in endocytosis and recycling in CHO cells on a time scale of <20 min as it displayed the same kinetics as transferrin recycling (Mayor et al., 1993; Presley et al., 1993). Endocytosis and recycling of C_6-NBD-SM have been quantitatively characterized in fibroblasts (see Koval and Pagano, 1991) and under a fluorescence microscope C_6-NBD-SM and C_6-NBD-GlcCer followed the endocytotic recycling pathway in differentiated HT29 epithelial cells (Kok et al., 1991). In these studies very little of the marker was delivered to the lysosomes. Also in MDCK, 85–90% of endocytosed marker reappeared on the cell surface in 1 h (Table I). In striking contrast, it has been observed in MDCK I that af-

ter basolateral endocytosis 73% of fluid-phase marker was transported to later endocytotic compartments (Bomsel et al., 1989).

In both MDCK lines, endocytosis of lipid per surface area (percentage endocytosis, Table I) was higher from the basolateral surface. In contrast, fluid-phase endocytosis per surface area was similar from both surfaces (von Bonsdorff et al., 1985; Bomsel et al., 1989). The two observations can only be true if basolateral endocytotic vesicles are smaller than apical ones, with a higher membrane to volume ratio. A similar discrepancy was observed in the ratio of transcytosis versus recycling from the basolateral endosomes. While 5–10 times more of the membrane marker recycled than transcytosed (Table I), the amounts of fluid phase in the two pathways were similar (Bomsel et al., 1989). Again this can only be true if recycling vesicles are smaller than transcytotic vesicles. The discrepancy was less for apical endosomes. While transcytosis was about 0.7 times recycling for the membrane marker (Table I), it was similar for fluid phase (Bomsel et al., 1989), arguing that apical recycling vesicles are not much smaller than transcytotic vesicles. The size of transcytotic vesicles in both directions must be the same because they transport the same amounts of membrane and fluid phase. So, like endocytotic vesicles, recycling vesicles on the basolateral side are smaller than apical ones.

In addition to higher rates of membrane endocytosis and recycling, the amount of C_6-NBD-GalCer in the cell (percentage intracellular, Fig. 2) was higher during transport from the basolateral than from the apical surface over a 6-h period. This indicates that the surface area of the endosomes as compared with the surface is greater on the basolateral side. In summary, the evidence suggests that membrane endocytosis and recycling are faster on the basolateral side, are mediated by smaller vesicles and involve larger endosomes.

Recently, it has been observed that material transcytosed from the basolateral surface after leaving the basolateral endosomes passes through an apically located recycling compartment before reaching the apical surface (Barroso and Sztul, 1994; see Mostov and Cardone, 1995). This would imply that membrane and fluid phase from the basolateral surface are recycled to that surface from two locations, the basolateral and apical endosomes. C_6-NBD-GalCer transcytosis in these MDCK II cells, from the same origin as ours but transfected with the polymeric Ig receptor (Mostov and Deitcher, 1986), was identical to that in the parental MDCK II (not shown).

Sphingolipid Sorting After Biosynthesis

After intracellular synthesis C_6-NBD-GlcCer, -SM, and -GalCer reached the surface of MDCK cells with different apical/basolateral polarities. As compared with the two other lipids, C_6-NBD-GlcCer was enriched twofold on the apical surface (Table III). As endogenous GlcCer in MDCK displayed a surface polarity 2.3 times higher than that of GalCer (Nichols et al., 1988), the selectivity in the transport of newly synthesized C_6-NBD-GlcCer and -GalCer appears sufficient to establish the different distribution of the native lipids at steady state. This has also been observed for C_6-NBD-GlcCer and -SM in intestinal cells (van 't Hof and van Meer, 1990; van't Hof et al., 1992). Only trace amounts of C_6-NBD-GalCer were synthesized. Similar relative rates of synthesis were observed for endogenous sphingolipids. Still, GalCer is a major glycolipid in MDCK II cells, constituting 15% of the glycolipids in these cells, about half as much as GlcCer (Brändli et al., 1988). Its low rate of synthesis suggests that GalCer is metabolically much more stable than GlcCer. More recently, synthesis of a major amount of short-chain GalCer (plus SM and GlcCer) was accomplished by applying a ceramide containing a hydroxy fatty acid. The polarity data in those experiments support the present data (van der Bijl, P., M. Lopes-Cardozo, and G. van Meer, manuscript submitted for publication).

Absence of Lipid Sorting During Transcytosis?

In contrast to the differential targeting of newly synthesized short-chain lipids, C_6-NBD-GlcCer was not sorted from C_6-NBD-SM during subsequent transcytosis, nor was it sorted from C_6-NBD-GalCer after insertion of the two lipids into either cell surface. The lack of sorting of NBD lipids in the transcytotic pathway could reflect a general lack of lipid sorting along this pathway. If so, differences in surface polarity between native lipids generated by the exocytotic transport would be dissipated by the transcytotic route. In that case, the exocytotic sorting of endogenous lipids must be more efficient than that of the C_6-NBD-analogues: in the absence of transcytotic lipid sorting the relative polarity of 2.6 between C_6-NBD-GlcCer and -GalCer, that had been generated after biosynthesis (cf. Table III), seems insufficient to maintain the relative polarity of 2.3 observed for endogenous GlcCer and GalCer in MDCK II (Nichols et al., 1988). Alternatively, the lack of sorting of NBD lipids could be an artifact of the C_6-NBD chain. In a confluent cell monolayer transcytosis probably contributes more to the equilibrium surface polarity of each lipid than transport of newly synthesized lipid. In equilibrium (Table II), transcytosis will transport 7% of the total cellular C_6-NBD-GlcCer per hour in each direction, while, if transport of newly synthesized lipid would only replace hydrolyzed lipid (2–4% of C_6-NBD-GlcCer per hour), it would deliver only 1–2% of the total C_6-NBD-GlcCer per hour to each cell surface. While new assays will have to be developed to address this issue, the NBD-lipid experiments show that lipid transport after cellular synthesis and lipid transcytosis do not possess the same sorting characteristics.

In one model for the mechanism by which newly synthesized lipids are targeted to the two epithelial cell surfaces with different apical/basolateral polarities (van Meer et al., 1987; Simons and van Meer, 1988), the lipids to be sorted pass through the lumenal leaflet of the membrane of the TGN. There they would be laterally segregated into (micro)domains that would subsequently bud into transport vesicles destined for either the apical or basolateral cell surface. If the model is correct, the absence of the sorting of NBD lipids during transcytosis implies that most transcytotic traffic does not involve the TGN or Golgi complex. Transport of short-chain GlcCer from the cell surface to the Golgi complex has been observed in nonepithelial cells (Martin and Pagano, 1994) and in undifferenti-

ated but not in differentiated HT29 epithelial cells (Kok et al., 1991). In the present study, we observed a punctate pattern of NBD fluorescence that did not resemble a Golgi pattern (van Meer et al., 1987; van 't Hof and van Meer, 1990) at any stage of the experiments (not shown).

Independent of whether the C_6-NBD lipids truly reflect the behavior of the endogenous lipids, the absolute values of membrane flux during transcytosis calculated here can be used to assess whether a specific protein is sorted or follows bulk flow. In addition, the influence of various conditions on the membrane fluxes along the transcytotic pathway can be studied, and it can be tested whether a change in transcytotic rate of a protein is specific for that protein or reflects a change in the size of the transcytotic pathway in general. Data generated by these approaches will contribute to our understanding of the principles of protein sorting in transcytotic organelles.

Dr. Wouter van 't Hof (now at Memorial Sloan Kettering Cancer Center, New York) carried out preliminary experiments and Ardy van Helvoort performed serine labeling for which they are gratefully acknowledged. We are grateful to Drs. Gerald Apodaca, James Casanova, Walter Hunziker, Karl Matlin, Keith Mostov, and Petra van der Bijl for positive suggestions and for providing us with cell lines. We thank Drs. Mark Marsh, Koert Burger, and the reviewers for critical comments on the manuscript, and Marion Thielemans for expert technical assistance.

Received for publication 3 January 1995 and in revised form 31 May 1995.

References

Aroeti, B., and K. E. Mostov. 1994. Polarized sorting of the polymeric immunoglobulin receptor in the exocytotic and endocytotic pathways is controlled by the same amino acids. *EMBO (Eur. Mol. Biol. Organ.) J.* 13:2297–2304.

Aroeti, B., P. A. Kosen, I. D. Kuntz, F. E. Cohen, and K. E. Mostov. 1993. Mutational and secondary structural analysis of the basolateral sorting signal of the polymeric immunoglobulin receptor. *J. Cell Biol.* 123:1149–1160.

Barroso, M., and E. S. Sztul. 1994. Basolateral to apical transcytosis in polarized cells is indirect and involves BFA and trimeric G protein sensitive passage through the apical endosome. *J. Cell Biol.* 124:83–100.

Bligh, E. G., and W. J. Dyer. 1959. A rapid method of total lipid extraction and purification. *Can. J. Biochem. Physiol.* 37:911–917.

Bomsel, M., K. Prydz, R. G. Parton, J. Gruenberg, and K. Simons. 1989. Endocytosis in filter-grown Madin-Darby canine kidney cells. *J. Cell Biol.* 109: 3243–3258.

Brändli, A. W., G. C. Hansson, E. Rodriguez-Boulan, and K. Simons. 1988. A polarized epithelial cell mutant deficient in translocation of UDP-galactose into the Golgi complex. *J. Biol. Chem.* 263:16283–16290.

Brändli, A. W., R. G. Parton, and K. Simons. 1990. Transcytosis in MDCK cells: identification of glycoproteins transported bidirectionally between both plasma membrane domains. *J. Cell Biol.* 111:2909–2921.

Butor, C., and J. Davoust. 1992. Apical to basolateral surface area ratio and polarity of MDCK cells grown on different supports. *Exp. Cell Res.* 203:115–127.

Casanova, J. E., P. P. Breitfeld, S. A. Ross, and K. E. Mostov. 1990. Phosphorylation of the polymeric immunoglobulin receptor required for its efficient transcytosis. *Science (Wash. DC).* 248:742–745.

Demel, R. A., and B. de Kruijff. 1976. The function of sterols in membranes. *Biochim. Biophys. Acta.* 457:109–132.

Fuller, S., C.-H. von Bonsdorff, and K. Simons. 1984. Vesicular stomatitis virus infects and matures only through the basolateral surface of the polarized epithelial cell line, MDCK. *Cell.* 38:65–77.

Hubbard, A. L., B. Stieger, and J. R. Bartles. 1989. Biogenesis of endogenous plasma membrane proteins in epithelial cells. *Annu. Rev. Physiol.* 51:755–770.

Hunziker, W., P. Mâle, and I. Mellman. 1990. Differential microtubule requirements for transcytosis in MDCK cells. *EMBO (Eur. Mol. Biol. Organ.) J.* 9: 3515–3525.

Kean, E. L. 1966. Separation of gluco- and galactocerebrosides by means of borate thin-layer chromatography. *J. Lipid Res.* 7:449–452.

Kok, J. W., T. Babia, and D. Hoekstra. 1991. Sorting of sphingolipids in the endocytic pathway of HT29 cells. *J. Cell Biol.* 114:231–239.

Koval, M., and R. E. Pagano. 1991. Intracellular transport and metabolism of sphingomyelin. *Biochim. Biophys. Acta.* 1082:113–125.

Lipsky, N. G., and R. E. Pagano. 1985. Intracellular translocation of fluorescent sphingolipids in cultured fibroblasts: endogenously synthesized sphingomyelin and glucocerebroside analogues pass through the Golgi apparatus en route to the plasma membrane. *J. Cell Biol.* 100:27–34.

Louvard, D. 1980. Apical membrane aminopeptidase appears at sites of cell-cell contact in cultured epithelial cells. *Proc. Natl. Acad. Sci. USA.* 77:4132–4136.

Martin, O. C., and R. E. Pagano. 1994. Internalization and sorting of a fluorescent analogue of glucosylceramide to the Golgi apparatus of human skin fibroblasts: utilization of endocytic and nonendocytic transport mechanisms. *J. Cell Biol.* 125:769–781.

Matter, K., J. A. Whitney, E. M. Yamamoto, and I. Mellman. 1993. Common signals control low density lipoprotein receptor sorting in endosomes and the Golgi complex of MDCK cells. *Cell.* 74:1053–1064.

Mayor, S., J. F. Presley, and F. R. Maxfield. 1993. Sorting of membrane components from endosomes and subsequent recycling to the cell surface occurs by a bulk flow process. *J. Cell Biol.* 121:1257–1269.

Mellman, I., E. Yamamoto, J. A. Whitney, M. Kim, W. Hunziker, and K. Matter. 1993. Molecular sorting in polarized and non-polarized cells: Common problems, common solutions. *J. Cell Sci. Suppl.* 17:1–7.

Mostov, K. E., and M. H. Cardone. 1995. Regulation of protein traffic in polarized epithelial cells. *Bioessays.* 17:129–138.

Mostov, K. E., and D. L. Deitcher. 1986. Polymeric immunoglobulin receptor expressed in MDCK cells transcytoses IgA. *Cell.* 46:613–621.

Nichols, G. E., T. Shiraishi, and W. W. Young, Jr. 1988. Polarity of neutral glycolipids, gangliosides, and sulfated lipids in MDCK epithelial cells. *J. Lipid Res.* 29:1205–1213.

Oka, J. A., and P. H. Weigel. 1989. The pathways for fluid phase and receptor mediated endocytosis in rat hepatocytes are different but thermodynamically equivalent. *Biochem. Biophys. Res. Commun.* 159:488–494.

Parton, R. G., K. Prydz, M. Bomsel, K. Simons, and G. Griffiths. 1989. Meeting of the apical and basolateral endocytic pathways of the Madin-Darby canine kidney cell in late endosomes. *J. Cell Biol.* 109:3259–3272.

Presley, J. F., S. Mayor, K. W. Dunn, L. S. Johnson, T. E. McGraw, and F. R. Maxfield. 1993. The *End2* mutation in CHO cells slows the exit of transferrin receptors from the recycling compartment but bulk membrane recycling is unaffected. *J. Cell Biol.* 122:1231–1241.

Prydz, K., S. H. Hansen, K. Sandvig, and B. van Deurs. 1992. Effects of brefeldin A on endocytosis, transcytosis and transport to the Golgi complex in polarized MDCK cells. *J. Cell Biol.* 119:259–272.

Rodriguez-Boulan, E., and W. J. Nelson. 1989. Morphogenesis of the polarized epithelial cell phenotype. *Science (Wash. DC).* 245:718–725.

Simons, K., and G. van Meer. 1988. Lipid sorting in epithelial cells. *Biochemistry.* 27:6197–6202.

Song, W., M. Bomsel, J. Casanova, J.-P. Vaerman, and K. Mostov. 1994. Stimulation of transcytosis of the polymeric immunoglobulin receptor by dimeric IgA. *Proc. Natl. Acad. Sci. USA.* 91:163–166.

Sztul, E., A. Kaplin, L. Saucan, and G. Palade. 1991. Protein traffic between distinct plasma membrane domains: isolation and characterization of vesicular carriers involved in transcytosis. *Cell.* 64:81–89.

Tomoda, H., Y. Kishimoto, and Y. C. Lee. 1989. Temperature effect on endocytosis and exocytosis by rabbit alveolar macrophages. *J. Biol. Chem.* 264: 15445–15450.

van Deurs, B., S. H. Hansen, O. W. Petersen, E. Løkken Melby, and K. Sandvig. 1990. Endocytosis, intracellular transport and transcytosis of the toxic protein ricin by a polarized epithelium. *Eur. J. Cell Biol.* 51:96–109.

van Genderen, I. L., and G. van Meer. 1993. Lipid sorting: measurement and interpretation. *Biochem. Soc. Trans.* 21:235–239.

van Genderen, I. L., G. van Meer, J. W. Slot, H. J. Geuze, and W. F. Voorhout. 1991. Subcellular localization of Forssman glycolipid in epithelial MDCK cells by immuno-electronmicroscopy after freeze-substitution. *J. Cell Biol.* 115:1009–1019.

van Helvoort, A. L. B., W. van't Hof, T. Ritsema, A. Sandra, and G. van Meer. 1994. Conversion of diacylglycerol to phosphatidylcholine on the basolateral surface of epithelial (MDCK) cells. Evidence for the reverse action of the sphingomyelin synthase. *J. Biol. Chem.* 269:1763–1769.

van Meer, G., and W. van't Hof. 1993. Epithelial sphingolipid sorting is insensitive to reorganization of the Golgi by nocodazole, but is abolished by monensin in MDCK cells and by brefeldin A in Caco-2 cells. *J. Cell Sci.* 104:833–842.

van Meer, G., E. H. K. Stelzer, R. W. Wijnaendts-van-Resandt, and K. Simons. 1987. Sorting of sphingolipids in epithelial (Madin-Darby canine kidney) cells. *J. Cell Biol.* 105:1623–1635.

van 't Hof, W., and G. van Meer. 1990. Generation of lipid polarity in intestinal epithelial (Caco-2) cells: sphingolipid synthesis in the Golgi complex and sorting before vesicular traffic to the plasma membrane. *J. Cell Biol.* 111: 977–986.

van 't Hof, W., J. Silvius, F. Wieland, and G. van Meer. 1992. Epithelial sphingolipid sorting allows for extensive variation of the fatty acyl chain and the sphingosine backbone. *Biochem. J.* 283:913–917.

van Weely, S., M. Brandsma, A. Strijland, J. M. Tager, and J. M. Aerts. 1993. Demonstration of the existence of a second, non-lysosomal glucocerebrosidase that is not deficient in Gaucher disease. *Biochim. Biophys. Acta.* 1181: 55–62.

von Bonsdorff, C.-H., S. D. Fuller, and K. Simons. 1985. Apical and basolateral endocytosis in Madin-Darby canine kidney (MDCK) cells grown on nitrocellulose filters. *EMBO (Eur. Mol. Biol. Organ.) J.* 4:2781–2792.

Welling, L. W., and D. J. Welling. 1975. Surface areas of brush border and lateral cell walls in the rabbit proximal nephron. *Kidney Int.* 8:343–348.